BIOCHEMISTRY
including biophysical chemistry & molecular biology

Article

pubs.acs.org/biochemistry

Structural Characterization of a Trapped Folding Intermediate of Pyrrolidone Carboxyl Peptidase from a Hyperthermophile

Mineyuki Mizuguchi,*[,†] Makoto Takeuchi,[‡] Shinya Ohki,[‡] Yuko Nabeshima,[†] Takahide Kouno,[†] Tomoyasu Aizawa,[§] Makoto Demura,[§] Keiichi Kawano,[§] and Katsuhide Yutani[⊥]

[†]Faculty of Pharmaceutical Sciences, University of Toyama, 2630, Sugitani, Toyama 930-0194, Japan

[‡]School of Materials Science, Japan Advanced Institute of Science and Technology, 1-1 Asahidai, Nomi, Ishikawa 923-1292, Japan

[§]Division of Biological Sciences, Graduate School of Science, Hokkaido University, Sapporo 060-0810, Japan

[⊥]RIKEN SPring-8 Center, RIKEN Harima Institute, 1-1-1 Kouto, Sayo, Hyogo 679-5148 Japan

Supporting Information

ABSTRACT: The refolding of cysteine-free pyrrolidone carboxyl peptidase (PCP-0SH) from a hyperthermophile is unusually slow. PCP-0SH is trapped in the denatured (D1) state at 4 °C and pH 2.3, which is different from the highly denatured state in the presence of concentrated denaturant. In order to elucidate the mechanism of the unusually slow folding, we investigated the structure of the D1 state using NMR techniques with amino acid selectively labeled PCP-0SH. The HSQC spectrum of the D1 state showed that most of the resonances arising from the 114−208 residues are broadened, indicating that conformations of the 114−208 residues are in intermediate exchange on the microsecond to millisecond time scale. Paramagnetic relaxation enhancement data indicated the lack of long-range interactions between the 1−113 and the 114−208 segments in the D1 state. Furthermore, proline scanning mutagenesis showed that the 114−208 segment in the D1 state forms a loosely packed hydrophobic core composed of α4- and α6-helices. From these findings, we conclude that the 114−208 segment of PCP-0SH folds into a stable compact structure with non-native helix−helix association in the D1 state. Therefore, in the folding process from the D1 state to the native state, the α4- and α6-helices become separated and the central β-sheet is folded between these helices. That is, the non-native interaction between the α4- and α6-helices may be responsible for the unusually slow folding of PCP-0SH.

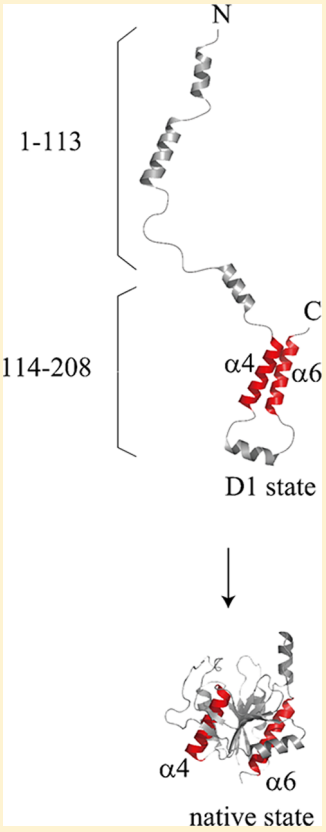

The mechanism by which a polypeptide chain folds into a native tertiary structure remains to be elucidated. The folding of a monomeric protein usually occurs on the order of milliseconds to seconds. A number of proteins fold into the native conformation through the folding intermediate, which is transiently formed at the early stage of folding.[1−3] The transient folding intermediate is often similar to the equilibrium molten globule state, which is a partially folded state with native-like secondary structure without extensive tertiary interactions. The molten globule state has been studied in detail for a number of globular proteins, including myoglobin, cytochrome *c*, α-lactalbumin, and β-lactoglobulin.[3] The folding intermediates of these proteins are suggested to be important for the efficient folding to the native conformation.[1,3]

In contrast to the efficient folding, several proteins refold very slowly, over a period ranging from minutes to hours. Although the efficient folding has been studied extensively, there is little research on the slow folding. Under some conditions, the slow folding is caused by the trapped folding intermediate, which precludes the formation of a native

Received: May 9, 2012
Revised: July 10, 2012
Published: July 16, 2012

ACS Publications © 2012 American Chemical Society

dx.doi.org/10.1021/bi300608e | *Biochemistry* 2012, 51, 6089−6096

structure. The trapped intermediates are potentially prone to aggregate due to incorrectly folded conformations containing the solvent-exposed hydrophobic surfaces.[4] In living biological systems, the trapped intermediates are recognized by regulatory systems such as molecular chaperones and degradation mechanisms.[5,6] Failure of such regulatory systems is one of the major factors in the formation of various harmful aggregates, including amyloid fibrils and cytotoxic oligomers.[4] Therefore, characterization of the trapped intermediates is important for elucidating the initiation of various misfolding diseases.

The slow folding proteins include ribonuclease T1, apo-plastocyanin, β2-microglobulin, and pyrrolidone carboxyl peptidase (PCP) from a hyperthermophile.[7−12] These proteins have at least one *cis*-proline residue in their native conformations, and prolyl trans-to-cis isomerization seems to be coupled with the slow folding. The rate constants of the slow folding of S54G/P55N ribonuclease T1 and β2-microglobulin are 0.4 h^{-1} at 10 °C and 0.5 h^{-1} at 4 °C, respectively.[7,10] The refolding of apo-plastocyanin is slower: the rate constant is 0.05 h^{-1} at 10 °C.[9] The trapped intermediate of apo-plastocyanin with an incorrect trans proline adopts a molten globule-like conformation, which fluctuates on the microsecond to millisecond time scale.[9] On the other hand, the intermediates of S54G/P55N ribonuclease T1 and β2-microglobulin have a native-like conformation.[7,10]

PCP is an enzyme which removes the L-pyroglutamic acid at the amino terminus of proteins. PCP is a homotetramer, and its monomer subunit adopts a single α/β globular fold.[13] The monomer has a central β-sheet composed of seven β-strands (β1, β2, β3 β4, β5, β8, and β9), a short two-stranded antiparallel β-sheet (β6 and β7), and six α-helices (α1 to α6). The central β-sheet is sandwiched by five α-helices: two α-helices (α2 and α4) on one side and three α-helices (α1, α3, and α6) on the other side (Figure 1).

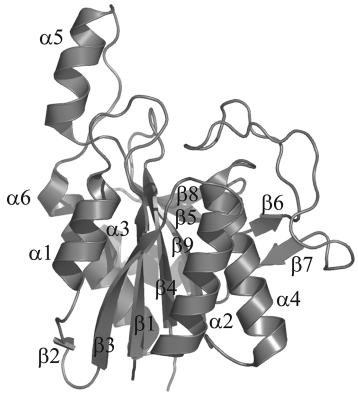

Figure 1. A ribbon representation of PCP-0SH drawn with PyMOL. Six α-helices and nine β-strands are labeled.

Cysteine-free PCP with Cys144Ser/Cys188Ser mutations (PCP-0SH) from *Pyrococcus furiosus*, a hyperthermophile exists as a homotetramer at neutral pH, and dissociates to a monomer at below pH 2.7.[14] The monomer at below pH 2.7 maintains the native conformation, enabling the detailed structural characterization of the monomer during the folding process, without considering the tetramerization. Iimura et al. have shown that the monomer at pH 2.5 has secondary and tertiary structures almost identical to those of the tetramer at pH 7.0.[15]

At pH below 2.7, PCP-0SH refolds very slowly from the highly denatured (D2) state to the native (N) state.[11,12] Before folding to the N state, the denatured (D1) state, corresponding to a folding intermediate, is formed at the early stage of refolding.[12] The refolding of PCP-0SH is too slow to be explained only by the prolyl trans-to-cis isomerization.[12] The refolding rate strongly depends on the temperature. At 40 °C and pH 2.3, the rate constant for the refolding is 0.3 h^{-1}, while the rate constant is 0.02 h^{-1} at 20 °C and pH 2.3.[11] At 5 °C and pH 2.3, PCP-0SH can be trapped in the D1 state and the refolding does not proceed further, enabling us to investigate the D1 state with a variety of techniques.[11,12]

Structural characterization of the D1 state is essential for elucidating the unusually slow folding of PCP-0SH. In the present study, we characterized the D1 state of PCP-0SH at pH 2.3 and 5 °C using nuclear magnetic resonance (NMR), circular dichroism (CD), and 8-anilinonaphthalene-1-sulfonate (ANS) fluorescence. Our results demonstrate that PCP-0SH adopts molten globule-like conformations with a loosely packed hydrophobic core composed of α4- and α6-helices. The α4- and α6-helices are within the 113−208 segment, which folds into an independent structural unit in the D1 state.

MATERIALS AND METHODS

Protein Expression and Purification. PCP-0SH was expressed in *Escherichia coli* strain JM109 using a protocol similar to that described previously.[14] The cells were resuspended in 50 mM Tris-HCl (pH 7.5), followed by sonication on ice. After the sonication, the suspension was heated at 95 °C for 10 min, and the aggregated materials were removed by centrifugation at 12 000 rpm for 30 min at 4 °C. The supernatant was applied to a DEAE Sepharose Fast Flow column (GE Healthcare), and the eluted protein was further purified by high-performance liquid chromatography (HPLC). M9 minimal medium substituted with the appropriate labeled compounds ([^{15}N]ammonium chloride and [^{13}C]glucose) was used for ^{15}N and ^{13}C labeling of protein. M9 medium made up with $^{2}H_2O$ in place of H_2O was used to prepare the ^{2}H/^{13}C/^{15}N-labeled protein.

We prepared the expression vectors of mutants of PCP-0SH using a QuikChange Site-Directed Mutagenesis Kit (Stratagene). DNA sequencing was conducted by using an ABI PRISM 3100 Genetic Analyzer (Applied Biosystems).

We performed amino acid selective labeling of PCP-0SH using a cell-free expression system.[16] ^{15}N-labeled amino acids were purchased from Cambridge Isotope Laboratories Inc. (Andover, MA). The DNA fragment encoding PCP-0SH with a stop codon was inserted into the NdeI and SalI sites of the pIVEX 2.3 vector (Roche Applied Science). The pIVEX 2.3 vector was used in the cell-free expression system of an RTS 500 ProteoMaster *E. coli* HY Kit.[16] The *in vitro* transcription and translation was performed using the RTS ProteoMaster Instrument according to the manufacturer's manual (Roche Applied Science).

The fragment of PCP-0SH corresponding to residues 113−208 was obtained as described previously.[17] After cell lysis by sonication, the 113−208 fragment was detected in the insoluble fraction. Protein purification was performed with anion-exchange chromatography and reverse-phase HPLC.[17] Matrix-assisted laser desorption ionization time-of-flight mass spectrometry showed that the 113−208 fragment has no methionine at the N-terminus.

Sample Preparation for the NMR, CD, and Fluorescence Experiments. PCP-0SH was dissolved in a solution containing 50 mM KCl and 6.0 M guanidine hydrochloride (GdnHCl) at pH 2.3, and the solution was incubated at 37 °C for 12 h. GdnHCl was removed by dialysis against 50 mM KCl (pH 2.3) at 4 °C. Under this condition, PCP-0SH can be trapped in the D1 state, and the refolding of PCP-0SH does not proceed further.[11,12] The solution was concentrated using an Amicon Ultra centrifugal filter device (10 kDa cutoff; Millipore) at 4 °C and used for the subsequent experiments.

NMR Experiments. The ^{15}N-labeled or ^{2}H/^{13}C/^{15}N-labeled PCP-0SH was prepared for the NMR experiments. The HSQC spectra were recorded on a Bruker DMX500, Varian INOVA750 or Bruker Avance800 spectrometer at 5 °C. Backbone resonances of the D1 state were assigned sequence specifically by analyzing three-dimensional TROSY-type spectra including TROSY-HNCA, -HN(CO)CA, -HNCO, -HN(CA)-CO, -HNCACB, and -HN(CO)CACB.[18,19] These spectra were acquired on a Varian INOVA750 spectrometer at 5 °C with deuterium decoupling. Protein concentrations were set to be 1.0 mM for the TROSY-type three-dimensional spectra. NMR data were processed using NMRPipe and analyzed using NMRView.[20,21]

Spin-labeling of PCP-0SH was performed as described previously.[22] PCP-0SH was labeled with the 3-(methanesulfonylthiomethyl)-2,2,5,5-tetramethylpyrrolidin-1-yloxy radical and purified by HPLC.[23]

Circular Dichroism. CD spectra were measured using a Jasco J-805 spectropolarimeter (JASCO Inc.). The temperature of the measuring cell was maintained at 5 °C by circulating water. Sample solutions contained 21−49 μM PCP-0SH and 50 mM KCl (pH 2.3). Protein concentrations were determined by the absorbance at 280 nm.

Fluorescence Spectroscopy. The hydrophobic fluorescent molecule, 1-anilino-8-naphthalenesulfonate (ANS), was used as a probe for detecting solvent-exposed hydrophobic residues.[24,25] Fluorescence spectra were recorded in an F-4500 fluorescence spectrometer (Hitachi). The temperature of the measuring cell was maintained at 5 °C by circulating water. The spectrometer was purged with N_2 gas to remove atmospheric H_2O. Fluorescence emission spectra between 400 and 650 nm were recorded with a fixed excitation wavelength of 380 nm. The bandwidths for excitation and emission were set to 10 and 20 nm, respectively. Sample solutions contained 25 μM ANS, 15 μM PCP-0SH, and 50 mM KCl (pH 2.3).

RESULTS

Previous studies have shown that PCP-0SH can be trapped in the D1 state at pH 2.3 and 5 °C, which differs from the D2 state in the presence of 6 M GdnHCl.[12] Figure 2 shows CD spectra of PCP-0SH in the N, D1, and D2 states at pH 2.3 and 5 °C. We analyzed the α-helix contents on the N and D1 states using the far-UV CD spectra.[26−29] As seen in Table 1, the D1 state retains α-helical contents almost identical to those of the N state.

A fully denatured protein usually gives close to zero near-UV CD signals. In contrast, the D1 state shows a mean residue ellipticity value of −38 deg cm^2 dmol^{-1} at 277 nm, which is probably attributable to the residual packing interaction of aromatic side chains (Figure 2B). This residual packing interaction is resistant to a high concentration of denaturant, since the D2 state also shows a significant near-UV CD signal (Figure 2B).

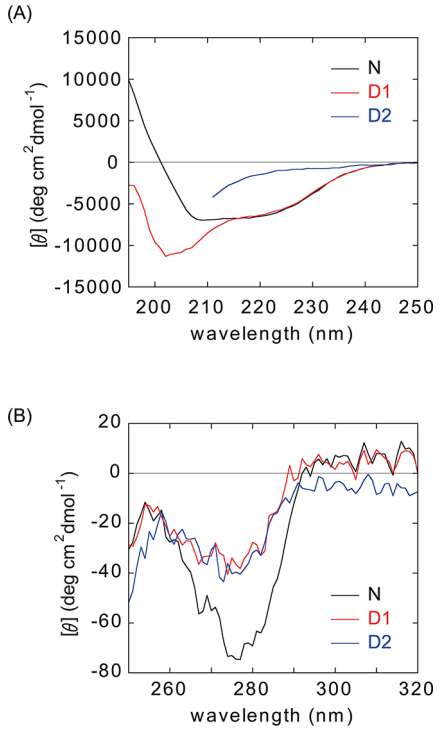

Figure 2. CD spectra of PCP-0SH at pH 2.3 and 5 °C in the (a) far- and (b) near-UV region. Black, red, and blue lines represent the CD spectra of PCP-0SH in the native (N), D1, and D2 state, respectively. The sample of the protein in the N state was obtained by dialysis of the protein solution at pH 7.0 against 50 mM KCl at pH 2.3. The sample of the protein in the D2 state contained 6 M GdnHCl and 50 mM KCl at pH 2.3.

Table 1. Helix Content of PCP-0SH Calculated from the Far-UV CD Spectra[a]

	helix content (%)			
N	19[b]	19[c]	16[d]	15[e]
D1	20[b]	17[c]	16[d]	9[e]

[a]The α-helix contents were calculated from the ellipticity values between 190 and 240 nm. [b]Obtained by the method of Sreerama and Woody.[26] [c]Obtained by the method of Provencher.[27] [d]Obtained by the method of Chen et al.[28] [e]Obtained by the method of Perez-Iratxeta and Andrade-Navarro.[29]

We investigated the structure of the D1 state using NMR techniques with amino acid selectively labeled PCP-0SH. The ^{1}H−^{15}N resonances of the D1 state are well resolved and have a narrow chemical shift dispersion typical of unfolded proteins (Figure 3). Conventional backbone resonance assignment was not applicable to the D1 state because only 91 resonances of 192 assignable residues were detectable. To overcome this difficulty, we performed amino acid selective isotope labeling of PCP-0SH using a cell-free expression system (Figure S1). The amino acid selective labeling enabled us to determine which type of amino acid gave rise to each resonance in the HSQC spectrum. We assigned 85 of 91 resonances in the HSQC using standard triple resonance experiments combined with amino acid selective labeling (Figure 3 and Figure S1). Intriguingly, all the assigned resonances originated from the residues 1−113 of PCP-0SH: the resonances of the residues 114−208 are hardly observed because of substantial resonance broadening. This means that the conformations of the residues 114−208 are in

dx.doi.org/10.1021/bi300608e | Biochemistry 2012, 51, 6089−6096

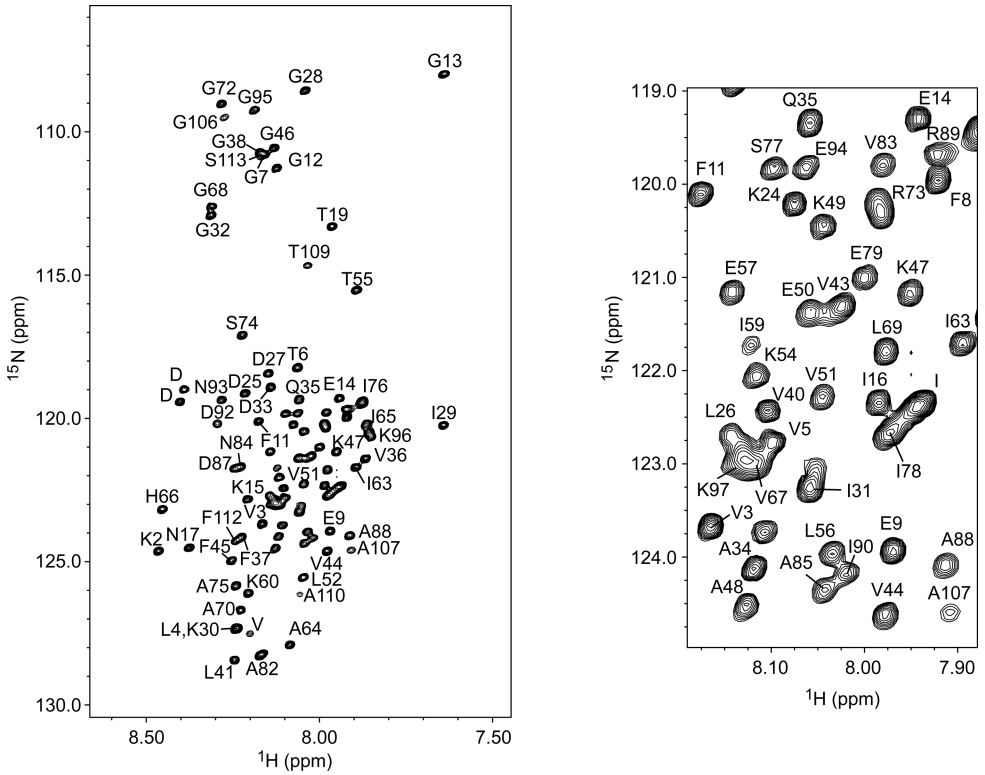

Figure 3. The 750 MHz ^{1}H−^{15}N HSQC spectrum of PCP-0SH in the D1 state at 5 °C. The sample contained 1.0 mM PCP-0SH and 50 mM KCl at pH 2.3. The backbone resonance assignments are indicated.

intermediate exchange on the NMR time scale.[30,31] In addition to the intermediate exchange, the resonance broadening might be caused by aggregation of proteins. However, since the D1 state exists as a monomer, the broadened resonances solely reflect the intermediate exchange of conformations on the NMR time scale.[30,31] Similar resonance broadening has been reported in the studies of the molten globule state of α-lactalbumin, which fluctuates in solution on the microsecond to millisecond time scale.[30,31] On the other hand, the residues 1−113 display sharp resonances with limited chemical shift dispersion of amide protons. This is diagnostic of the rapid interconversion on the NMR time scale between many different conformers without tertiary interactions.[32] These results indicate that the dynamic nature is quite different between the 1−113 segment and the 114−208 segment in the D1 state.

We next investigated the long-range interactions between the 1−113 segment and the 114−208 segment in the D1 state. The long-range interactions in an unfolded protein can be observed in paramagnetic relaxation enhancement (PRE) experiments.[22,33] PRE utilizes the spin-label nitroxide, which is conjugated to the thiol group of Cys by forming a disulfide bond. We substituted Cys for four residues (K122, H152, E172, or E194) to conjugate the protein with the spin-label nitroxide. The resonances of the amide proton can be attenuated when the distance of the $^{1}H^{N}$ and the spin-labeled site is within 25 Å.[22,33] The PRE effects (I_{para}/I_{dia}) can be evaluated by acquiring HSQC spectra in the oxidized and reduced state of the spin-label.

Spin-labeling at residue K122C leads to strong signal attenuation at position T109 and weak attenuation at G106 and A107. Other than these residues, there is no signal attenuation in the residues 1−113 (Figure 4). Spin-labeling at other positions showed similar PRE effects: the spin-labeling at H152, E172, and E194 did not reduce the intensities of the signals originating from the residues 1−113 in the D1 state (Figure 4). These results indicate that the 1−113 segment does not interact with the 114−208 segment in the D1 state.

We examined whether the D1 state maintains the α-helices formed in the N state. For this purpose, the secondary structure of the D1 state was investigated by using far-UV CD and proline scanning mutagenesis. As is well-known, proline mutation unfolds or greatly destabilizes the protein structure when inserted in the middle of secondary structures.[34] We targeted mutations to residues that are helical in the N state of PCP-0SH because numerous studies have shown that the folding intermediates contain native-like helices.[1−3] The effects of proline mutations on the secondary structure were evaluated by recording far-UV CD spectra (Figure S2). The Y147P and A199P substitutions reduced the secondary structure content, while the I178P substitution did not. Compared with Y147P and A199P mutations, the double mutation of Y147P/A199P greatly reduced the secondary structure content.

We recorded far-UV CD spectra of 16 proline mutants and summarized the mean residue ellipticities at 222 nm (Figure 5). All single mutations other than I178P reduced the secondary structure, indicating that the D1 state has a helical structure at these mutated positions. As described above, the I178P mutation has no effect on the secondary structure in the D1 state, but the mutation of the preceding K177 reduced the secondary structure. Therefore, K177 is included in a helix, while I178 is not in the helix in the D1 state. In the native tetramer, both K177 and I178 are included in the α5-helix.[13] On the other hand, a solution NMR study has shown that the α5-helix is partly destroyed in the native monomeric structure at pH 2.5.[15]

dx.doi.org/10.1021/bi300608e | *Biochemistry* 2012, 51, 6089−6096

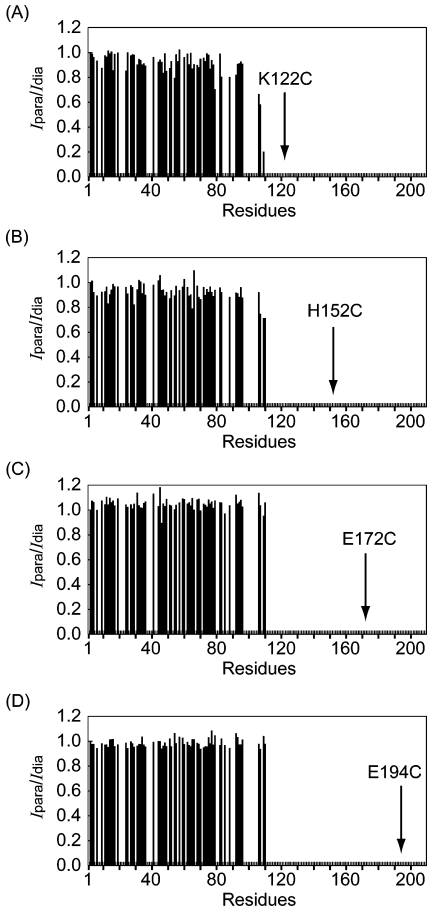

Figure 4. Paramagnetic enhancement of the nuclear spin relaxation for the D1 state of PCP-0SH at pH 2.3 and 5 °C. The histograms indicate the experimental intensity ratios (I_{para}/I_{dia}) for each residue with an adequately resolved resonance in the $^{1}H-^{15}N$ HSQC spectrum of the spin-labeled PCP-0SH with (a) K122C, (b) H152C, (c) E172C, and (d) E194C mutation. The HSQC signals of the residues 114−208 are broadened beyond detection (see text). An arrow indicates the spin-labeled location.

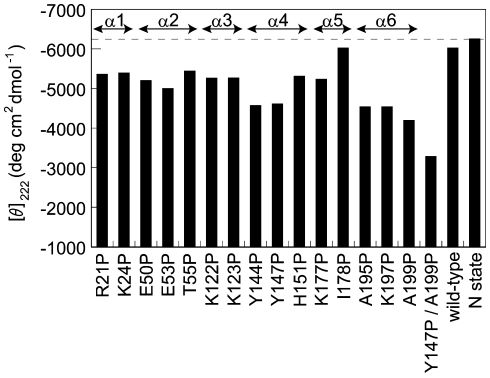

Figure 5. Effects of proline mutations on CD ellipticity at 222 nm of PCP-0SH in the D1 state. The CD spectra were recorded at 5 °C. Y147P/A199P designates the double mutation of Y147P and A199P. A dashed line represents the CD ellipticity at 222 nm of wild-type PCP-0SH in the N state at pH 2.3. The position of the α-helix is indicated at the top of the figure.

In general terms, the folding intermediate of globular proteins is often characterized by a loosely packed hydrophobic core.[2,3] In order to examine whether the D1 state of PCP-0SH has a loosely packed hydrophobic core, we investigated the D1 state using a fluorescent probe ANS, which binds to the hydrophobic cluster exposed to solvent.[24,25] The ANS fluorescence intensity observed for the D1 state was 7-fold higher than that for the N state (Figure 6A). This suggests that

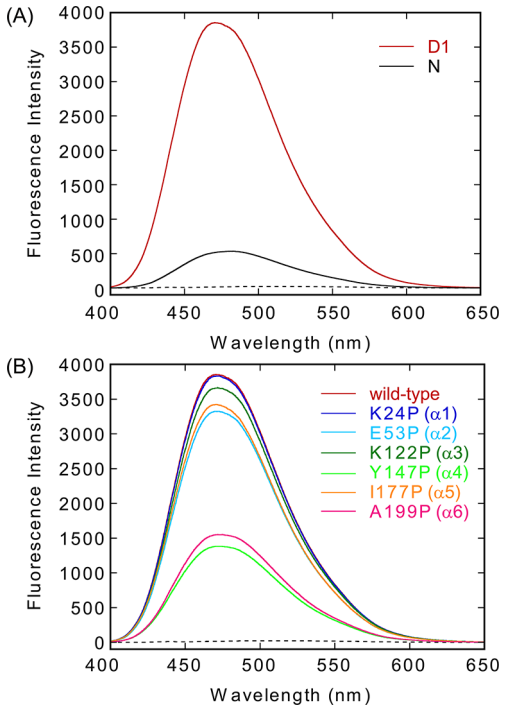

Figure 6. Fluorescence spectra of 25 μM ANS in the presence of PCP-0SH at pH 2.3. The ANS fluorescence spectra were recorded at 5 °C. A dashed line represents the fluorescence spectrum of 25 μM ANS. (A) Red, wild-type D1 state; black, wild-type N state. (B) Effects of proline mutations on ANS fluorescence of PCP-0SH in the D1 state. Red, wild-type; blue, K24P; cyan, E53P; green, K122P; light green, Y147P; orange, I177P; and pink, A199P.

the D1 state forms a molten globule-like structure consisting of an ensemble of loosely packed structures. It is known that the molten globule state is characterized by particularly high ANS fluorescence intensities due to the exposure of the hydrophobic cluster.[2,25] Extensive tight packing interactions in the native structure reduce the hydrophobic surface area that the ANS molecule gains access to (Figure 6A).[2,25]

We recorded ANS fluorescence spectra in the presence of the proline mutants in the D1 state (Figure 6B). The Y147P and A199P mutations dramatically reduced the ANS fluorescence, as compared with that in the presence of the wild-type D1 state. Therefore, unfolding of the α4- or α6-helix leads to disruption of the loosely packed hydrophobic core in the D1 state. In contrast, the K24P, E53P, K122P, and I177P mutations had little or no effect on the ANS fluorescence (Figure 6B).

To strengthen the conclusion described above, we investigated a fragment corresponding to the residues 113−208 of PCP-0SH. The 113−208 fragment has a secondary structure as judged by the far-UV-CD spectrum (Figure 7A). The ANS fluorescence spectra show that ANS strongly binds to the 113−208 fragment and that denaturation by GdnHCl reduces the ANS fluorescence intensity (Figure 7C). Furthermore, the $^{1}H-^{15}N$ HSQC spectrum of the fragment showed substantial resonance broadening (Figure 8). These results suggest that the 113−208 fragment adopts a molten

dx.doi.org/10.1021/bi300608e | Biochemistry 2012, 51, 6089−6096

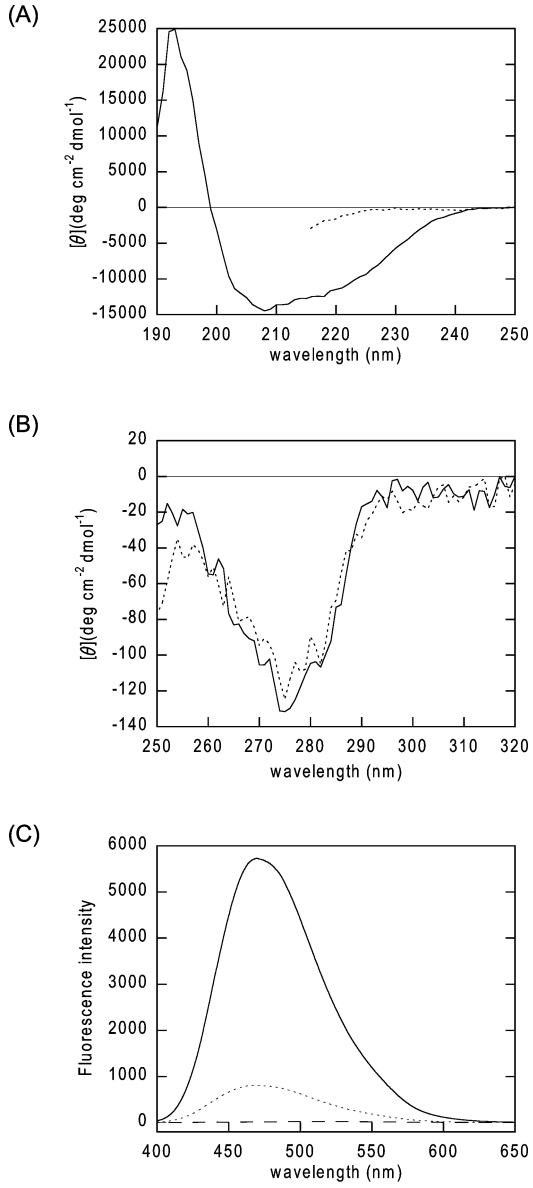

Figure 7. (A, B) CD spectra of the fragment corresponding to residues 113−208 of PCP-0SH in the (A) far-UV and (B) near-UV region in 50 mM KCl at pH 2.3 and 25 °C. Solid and dotted lines represent the CD spectra at 0 and 7 M GdnHCl, respectively. (C) ANS fluorescence of the fragment corresponding to residues 113−208 of PCP-0SH. Solid and dotted lines represent the ANS fluorescence spectra at 0 and 7 M GdnHCl, respectively. The dashed line represents the fluorescence spectrum of 25 μM ANS.

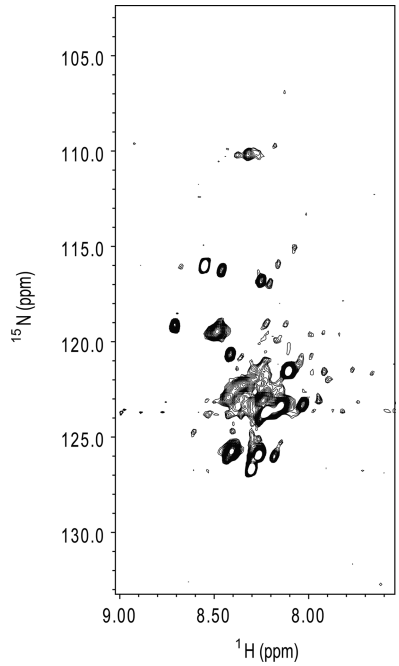

Figure 8. $^{1}H-^{15}N$ HSQC spectrum of the fragment corresponding to residues 113−208 of PCP-0SH. The spectrum was acquired using a Bruker Avance 800 MHz NMR spectrometer equipped with a cryoprobe at 25 °C.

globule-like conformation, which has a secondary structure with a loosely packed hydrophobic core.[1−3]

As seen in the near-UV CD spectrum of the full-length protein (Figure 2B), the fragment shows a strong signal in the near-UV CD region (Figure 7B). This is probably attributed to the residual packing interaction of aromatic side chains that is resistant to 7 M GdnHCl (Figure 7B).

Although the $^{1}H-^{15}N$ HSQC spectrum of the fragment showed substantial resonance broadening, some resonances are very intense in Figure 8. These intense resonances are not seen in the HSQC spectrum of the D1 state of PCP-0SH (Figure 3). This may result from the difference in the overall correlation time between the proteins. It is reasonable to consider that the D1 state of full-length PCP-0SH has a longer overall correlation time than the 113−208 fragment. The line widths are approximately proportional to the overall rotational correlation time: the sharp resonances are broadened, depending on the molecular weight and shape of the molecule.[35]

We can summarize our results as follows. The 113−208 segment of PCP-0SH folds into an independent structural unit in the D1 state. The 113−208 segment forms a molten globule-like structure consisting of an ensemble of loosely packed structures. The loosely packed hydrophobic core of the D1 state is composed of α4- and α6-helices, while the α4 and α6-helices have no contact with each other in the native structure: the central β-sheet is located between the helices (Figure 1).[13]

DISCUSSION

In the folding of many globular proteins, a molten globule-like folding intermediate is formed at the early stage of folding.[1−3] After the molten globule formation, proteins fold into the native structure with specific tertiary interactions. As described above, the molten globule state has a native-like secondary structure without an extensive tertiary structure. Furthermore, it has a compact structure with a loosely packed hydrophobic core and native-like backbone topology, namely, a native-like overall fold.[34] The native-like overall fold of the molten globule state brings side chains to the correct positions in three-dimensional space, leading to the specific tertiary interactions of the native proteins. The overall fold of the molten globule state is important for the folding from the molten globule state to the native state.[34]

Comparison of the D1 State with the Molten Globule State. We characterized the structure of the D1 state using NMR, CD and ANS fluorescence. Our results demonstrate that the D1 state is similar to the molten globule state; i.e., it has a native-like secondary structure and a loosely packed hydrophobic core. The Gibbs energy change of unfolding for the D1 state of PCP-0SH was 15.3 ± 0.7 kJ/mol at 5 °C (Figure S3),

dx.doi.org/10.1021/bi300608e | Biochemistry 2012, 51, 6089−6096

which is comparable to those for the molten globule state of other proteins like α-lactalbumin.[36−38] Proline scanning mutagenesis showed that the D1 state maintains native-like α-helices (α1 to α6), although these helices may be shorter than in the N state. The α4- and α6-helices are critical for the loosely packed hydrophobic core, while other helices are not included in the hydrophobic core. The α4- and α6-helices are composed of the residues 140−157 and the residues 188−205, respectively, and therefore the interactions within the 114−208 segment stabilize the loosely packed hydrophobic core. On the other hand, the 114−208 segment fluctuates on the microsecond to millisecond time scale, as judged by the substantial resonance broadening in the HSQC spectrum. Taken together, these results let us to conclude that the 114−208 segment folds into the molten globule-like state in the D1 state.

A previous study has shown that the overall backbone fold in the N state is retained in the molten globule state of α-lactalbumin.[34] Does the D1 state of PCP-0SH maintain the native-like fold like the α-lactalbumin molten globule? Judging from the X-ray crystal structure, the whole polypeptide chain of PCP-0SH folds into a single domain with complex fold pattern in the N state.[13] In contrast, the 114−208 segment forms the loosely packed core composed of α4- and α6-helices in the D1 state without interacting with the 1−113 segment. In addition, the D1 state is stabilized by non-native helix−helix association within the 114−208 segment (see below). Therefore, it is likely that the overall fold of the D1 state is different from that of the N state.

Non-native Helix−Helix Association in the D1 State. Previous studies have shown that the α6-helix is important for the folding and stability of PCP-0SH.[15,39] Disruption of the α6-helix by the A199P mutation reduced the stability and the refolding rate of PCP-0SH. NMR analysis combined with hydrogen−deuterium exchange revealed that the α6-helix is formed in the D1 state of PCP-0SH.[15] Furthermore, a peptide fragment corresponding to the α6-helix showed significant helical propensity, while a peptide with A199P mutation did not.[39]

Our results suggest that the loosely packed hydrophobic core in the D1 state is composed of α4- and α6-helices. In other words, the α4- and α6-helices loosely associate with each other and form the hydrophobic core in the D1 state. In contrast, in the native structure of PCP-0SH, the α4- and α6-helices have no contact with each other, since the α4- and α6-helices sandwich the central β-sheet composed of seven β-strands (β1, β2, β3, β4, β5, β8, and β9).[13] Among these β-strands, the β1 to β5 are located on the 1−113 segment in the N state. On the other hand, PRE experiments suggested the lack of long-range interactions between the 1−113 segment and the 114−208 segment containing the α4- and α6-helices in the D1 state. These results appear to show that the α4- and α6-helices become separated, and the central β-sheet is folded between these helices in a folding process from the D1 state to the N state. It is likely that the non-native interaction between the α4- and α6-helices is responsible for the slow folding of PCP-0SH.

The disruption of the non-native interactions by mutagenesis may accelerate the refolding of PCP-0SH. It has been shown that the disruption of the non-native aromatic and hydrophobic interaction significantly accelerates the refolding of hen egg lysozyme.[40] The rate-limiting step in the folding of lysozyme arises as a consequence of the formation of an intermediate which contains a significant non-native structure that must be disrupted prior to, or in concert with, subsequent folding.[40]

Ogasahara et al. have shown that the refolding rate of PCP-0SH is 3.3×10^2 h^{-1} at pH 7 and 25 °C, which is much higher than the value at pH 2.3: the refolding rate is 2.6×10^{-2} h^{-1} at pH 2.3 and 25 °C.[11,41] Furthermore, the refolding of PCP-0SH is explained by a two-state model at pH 7 and 60 °C: PCP-0SH refolds directly to the native tetramer without any intermediate state.[41] From these results, it seems that the non-native helix−helix interaction in the D1 state is stabilized by the protonation, and the refolding of PCP-0SH occurs much more slowly at pH 2.3. In order to fully understand the slow folding of PCP-0SH, it will be necessary to investigate how the non-native helix−helix interaction contributes to the energy barrier for the transition from the D1 state to the N state.

■ ASSOCIATED CONTENT

Ⓢ Supporting Information

Figures S1−S3. This material is available free of charge via the Internet at http://pubs.acs.org.

■ AUTHOR INFORMATION

Corresponding Author

*Tel +81-76-434-7595; Fax +81-76-434-5061; e-mail mineyuki@pha.u-toyama.ac.jp.

Funding

This study was supported by Grants-in-Aids for Scientific Research on Priority Areas from the Ministry of Education, Culture, Science and Technology of Japan.

Notes

The authors declare no competing financial interest.

■ ACKNOWLEDGMENTS

We thank Takara Bio Inc. for providing the PCP-0SH plasmid (pPCP3022).

■ ABBREVIATIONS

ANS, 8-anilinonaphthalene-1-sulfonate; CD, circular dichroism; GdnHCl, guanidine hydrochloride; PCP-0SH, cystein-free pyrrolidone carboxyl peptidase; PCP, pyrrolidone carboxyl peptidase; D1, denatured; D2, highly denatured; HPLC, high-performance liquid chromatography; N, native; NMR, nuclear magnetic resonance; PRE, paramagnetic relaxation enhancement.

■ REFERENCES

(1) Kuwajima, K. (1989) The molten globule state as a clue for understanding the folding and cooperativity of globular-protein structure. *Proteins 6*, 87−103.

(2) Ptitsyn, O. B. (1995) Molten globule and protein folding. *Adv. Protein Chem. 47*, 83−229.

(3) Arai, M., and Kuwajima, K. (2000) Role of the molten globule state in protein folding. *Adv. Protein Chem. 53*, 209−282.

(4) Dobson, C. M. (2003) Protein folding and misfolding. *Nature 426*, 884−890.

(5) Todd, M. J., Viitanen, P. V., and Lorimer, G. H. (1994) Dynamics of the chaperonin ATPase cycle: implications for facilitated protein folding. *Science 265*, 659−666.

(6) Kaufman, R. J., Scheuner, D., Schröder, M., Shen, X., Lee, K., Liu, C. Y., and Arnold, S. M. (2002) The unfolded protein response in nutrient sensing and differentiation. *Nat. Rev. Mol. Cell Biol. 3*, 411−421.

(7) Steegborn, C., Schneider-Hassloff, H., Zeeb, M., and Balbach, J. (2000) Cooperativity of a protein folding reaction probed at multiple chain positions by real-time 2D NMR spectroscopy. *Biochemistry 39*, 7910−7919.

(8) Koide, S., Dyson, H. J., and Wright, P. E. (1993) Characterization of a folding intermediate of apoplastocyanin trapped by proline isomerization. *Biochemistry 32*, 12299−12310.
(9) Mizuguchi, M., Kroon, G. J., Wright, P. E., and Dyson, H. J. (2003) Folding of a β-sheet protein monitored by real-time NMR spectroscopy. *J. Mol. Biol. 328*, 1161−1171.
(10) Kameda, A., Hoshino, M., Higurashi, T., Takahashi, S., Naiki, H., and Goto, Y. (2005) Nuclear magnetic resonance characterization of the refolding intermediate of β2-microglobulin trapped by non-native prolyl peptide bond. *J. Mol. Biol. 348*, 383−397.
(11) Kaushik, J, K., Ogasahara, K., and Yutani, K. (2002) The unusually slow relaxation kinetics of the folding-unfolding of pyrrolidone carboxyl peptidase from a hyperthermophile, *Pyrococcus furiosus*. *J. Mol. Biol. 316*, 991−1003.
(12) Iimura, S., Yagi, H., Ogasahara, K., Akutsu, H., Noda, Y., Segawa, S., and Yutani, K. (2004) Unusually slow denaturation and refolding processes of pyrrolidone carboxyl peptidase from a hyperthermophile are highly cooperative: real-time NMR studies. *Biochemistry 43*, 11906−11915.
(13) Tanaka, H., Chinami, M., Mizushima, T., Ogasahara, K., Ota, M., Tsukihara, T., and Yutani, K. (2001) X-ray crystalline structures of pyrrolidone carboxyl peptidase from a hyperthermophile, *Pyrococcus furiosus*, and its cys-free mutant. *J. Biochem. 130*, 107−118.
(14) Ogasahara, K., Khechinashvili, N. N., Nakamura, M., Yoshimoto, T., and Yutani, K. (2001) Thermal stability of pyrrolidone carboxyl peptidases from the hyperthermophilic Archaeon, *Pyrococcus furiosus*. *Eur. J. Biochem. 268*, 3233−3242.
(15) Iimura, S., Umezaki, T., Takeuchi, M., Mizuguchi, M., Yagi, H., Ogasahara, K., Akutsu, H., Noda, Y., Segawa, S., and Yutani, K. (2007) Characterization of the denatured structure of pyrrolidone carboxyl peptidase from a hyperthermophile under nondenaturing conditions: role of the C-terminal α-helix of the protein in folding and stability. *Biochemistry 46*, 3664−3672.
(16) Hoffmann, M., Nemetz, C., Madin, K., and Buchberger, B. (2004) Rapid translation system: a novel cell-free way from gene to protein. *Biotechnol. Annu. Rev. 10*, 1−30.
(17) Mizuguchi, M., Hayashi, A., Takeuchi, M., Dobashi, M., Mori, Y., Shinoda, H., Aizawa, T., Demura, M., and Kawano, K. (2008) Unfolding and aggregation of transthyretin by the truncation of 50 N-terminal amino acids. *Proteins 72*, 261−269.
(18) Salzmann, M., Pervushin, K., Wider, G., Senn, H., and Wüthrich, K. (1998) TROSY in triple-resonance experiments: new perspectives for sequential NMR assignment of large proteins. *Proc. Natl. Acad. Sci. U. S. A. 95*, 13585−13590.
(19) Salzmann, M., Wider, G., Pervushin, K., Senn, H., and Wüthrich, K. (1999) TROSY-type triple-resonance experiments for sequential NMR assignments of large proteins. *J. Am. Chem. Soc. 121*, 844−848.
(20) Delaglio, F., Grzesiek, S., Vuister, G. W., Zhu, G., Pfeifer, J., and Bax, A. (1995) NMRPipe: a multidimensional spectral processing system based on UNIX pipes. *J. Biomol. NMR 6*, 277−293.
(21) Johnson, B. A. (2004) Using NMR. View to visualize and analyze the NMR spectra of macromolecules. *Methods Mol. Biol. 278*, 313−352.
(22) Lietzow, M. A., Jamin, M., Dyson, H. J., and Wright, P. E. (2002) Mapping long-range contacts in a highly unfolded protein. *J. Mol. Biol. 322*, 655−662.
(23) Mchaourab, H. S., Kálai, T., Hideg, K., and Hubbell, W. L. (1999) Motion of spin-labeled side chains in T4 lysozyme: effect of side chain structure. *Biochemistry 38*, 2947−2955.
(24) Stryer, L. (1965) The interaction of a naphthalene dye with apomyoglobin and apohemoglobin. A fluorescent probe of non-polar binding sites. *J. Mol. Biol. 13*, 482−495.
(25) Semisotnov, G. V., Rodionova, N. A., Razgulyaev, O. I., Uversky, V. N., Gripas', A. F., and Gilmanshin, R. I. (1991) Study of the "molten globule" intermediate state in protein folding by a hydrophobic fluorescent probe. *Biopolymers 31*, 119−128.
(26) Sreerama, N., and Woody, R. W. (1993) A self-consistent method for the analysis of protein secondary structure from circular dichroism. *Anal. Biochem. 209*, 32−44.
(27) Provencher, S. W. (1982) CONTIN: a general purpose constrained regularization program for inverting noisy linear algebraic and integral equations. *Comput. Phys. Commun. 27*, 229−242.
(28) Chen, Y. H., Yang, J. T., and Chau, K. H. (1974) Determination of the helix and beta form of proteins in aqueous solution by circular dichroism. *Biochemistry 13*, 3350−3359.
(29) Perez-Iratxeta, C., and Andrade-Navarro, M. A. (2008) K2D2: estimation of protein secondary structure from circular dichroism spectra. *BMC Struct. Biol. 13*, 8−25.
(30) Baum, J., Dobson, C. M., Evans, P. A., and Hanley, C. (1989) Characterization of a partly folded protein by NMR methods: studies on the molten globule state of guinea pig α-lactalbumin. *Biochemistry 28*, 7−13.
(31) Alexandrescu, A. T., Evans, P. A., Pitkeathly, M., Baum, J., and Dobson, C. M. (1993) Structure and dynamics of the acid-denatured molten globule state of α-lactalbumin: a two-dimensional NMR study. *Biochemistry 32*, 1707−1718.
(32) Dyson, H. J., and Wright, P. E. (2004) Unfolded proteins and protein folding studied by NMR. *Chem. Rev. 104*, 3607−3622.
(33) Wu, K. P., Kim, S., Fela, D. A., and Baum, J. (2008) Characterization of conformational and dynamic properties of natively unfolded human and mouse α-synuclein ensembles by NMR: implication for aggregation. *J. Mol. Biol. 378*, 1104−1115.
(34) Schulman, B. A., and Kim, P. S. (1996) Proline scanning mutagenesis of a molten globule reveals non-cooperative formation of a protein's overall topology. *Nat. Struct. Biol. 3*, 682−687.
(35) Cavanagh, J., Fairbrother, W. J., Palmer, A. G., III, and Skelton, N. J. (1996) Classical NMR spectroscopy, in *Protein NMR spectroscopy: principles and practice*, 1st ed., pp 1−24, Academic Press, San Diego.
(36) Kuwajima, K., Nitta, K., Yoneyama, M., and Sugai, S. (1976) Three-state denaturation of α-lactalbumin by guanidine hydrochloride. *J. Mol. Biol. 106*, 359−373.
(37) Kuwajima, K. (1977) A folding model of α-lactalbumin deduced from the three-state denaturation mechanism. *J. Mol. Biol. 114*, 241−258.
(38) Nozaka, M., Kuwajima, K., Nitta, K., and Sugai, S. (1978) Detection and characterization of the intermediate on the folding pathway of human α-lactalbumin. *Biochemistry 17*, 3753−3758.
(39) Umezaki, T., Iimura, S., Noda, Y., Segawa, S., and Yutani, K. (2008) The confirmation of the denatured structure of pyrrolidone carboxyl peptidase under nondenaturing conditions: difference in helix propensity of two synthetic peptides with single amino acid substitution. *Proteins 71*, 737−742.
(40) Rothwarf, D. M., and Scheraga, H. A. (1996) Role of non-native aromatic and hydrophobic interactions in the folding of hen egg white lysozyme. *Biochemistry 35*, 13797−13807.
(41) Ogasahara, K., Nakamura, M., Nakura, S., Tsunasawa, S., Kato, I., Yoshimoto, T., and Yutani, K. (1998) The unusually slow unfolding rate causes the high stability of pyrrolidone carboxyl peptidase from a hyperthermophile, *Pyrococcus furiosus*: equilibrium and kinetic studies of guanidine hydrochloride-induced unfolding and refolding. *Biochemistry 37*, 17537−17544.